DiffECG: A Generalized Probabilistic Diffusion Model for ECG Signals Synthesis

Nour Neifar[1], Achraf Ben-Hamadou[2], Afef Mdhaffar[1], and Mohamed Jmaiel[1]

[1] ReDCAD Lab, ENIS, University of Sfax, Tunisia
{nour.neifar@redcad.org, afef.mdhaffar@enis.tn, mohamed.jmaiel@redcad.org
[2] Centre de Recherche en Numérique de Sfax, Laboratory of Signals, Systems, Artificial Intelligence and Networks, Technopôle de Sfax, Sfax, Tunisia
achraf.benhamadou@crns.rnrt.tn

Abstract. In recent years, deep generative models have gained attention as a promising data augmentation solution for heart disease detection using deep learning approaches applied to ECG signals. In this paper, we introduce a novel approach based on denoising diffusion probabilistic models for ECG synthesis that covers three scenarios: heartbeat generation, partial signal completion, and full heartbeat forecasting. Our approach represents the first generalized conditional approach for ECG synthesis, and our experimental results demonstrate its effectiveness for various ECG-related tasks. Moreover, we show that our approach outperforms other state-of-the-art ECG generative models and can enhance the performance of state-of-the-art classifiers.

Keywords: Generative models · diffusion model · ECG generation · ECG completion · ECG forecasting

1 Introduction

Cardiovascular diseases (CVDs) are the leading cause of death worldwide, underscoring the importance of diagnostic tools for monitoring heart health [19]. Electrocardiograms (ECG) represent the most significant non-invasive method for identifying cardiovascular problems [14]. ECG recordings capture the heart's electrical activity and are crucial for detecting various heart problems. However, sudden cardiac issues can make ECG recording challenging, and equipment failure and other factors can lead to missing ECG values. These issues can limit the effectiveness of deep learning techniques proposed for preventing CVDs. Data synthesis, completion and forecasting are well-known and effective solutions for addressing the challenges caused by missing or incomplete data. However, due to the complex dynamics of ECG signals, the synthesis of such signals is a challenging task [8, 7, 24, 22]. Recently, diffusion models have emerged as a highly effective class of deep generative models for these tasks [11, 26]. These models offer several advantages over Generative Adversarial Networks [9], such as training stability and the ability to generate diverse synthetic samples. Diffusion models have been shown to be effective in a wide range of applications, including image generation [5], video generation [12], and time series modeling [27, 2].

In this context, we propose a generalized framework based on Diffusion Denoising Probabilistic Models (DDPMs) for ECG signal generation, completion, and forecasting. Our contributions are as follows:

- We introduce the first generalized DDPM model for ECG signal generation, completion, and forecasting.
- We enable conditional generation for different classes of ECG signals.
- We effectively condition the reverse diffusion based on spectrogram representation of ECG signals to guide the ECG signal synthesis for all three tasks.

Our proposed approach is evaluated on the MIT-BIH arrhythmia database. Experimental results demonstrate the effectiveness of our method for generating, completion, and forecasting ECG signals with realistic morphology. Furthermore, augmenting the real training dataset with synthetic ECG signals generated by our method has significantly improved the state-of-the-art ECG arrhythmia classification performance.

The remainder of this paper is organized as follows: section 2 provides an overview of related work, section 3 details our proposed approach, section 4 presents the obtained experimental results, and finally, section 5 summarizes our contributions and outlines some future research directions.

2 Related work

This section provides an overview of current research on deep generative models applied to ECG signals, as well as an introduction to the basic principles of diffusion models.

2.1 Deep generative models applied to ECG

Several previous studies investigated the use of deep learning techniques for time series generation and completion, with deep generative models being a popular choice [29, 17, 18, 20]. GANs have been widely employed for the related ECG tasks [8, 7, 24, 22, 6]. The most recent advanced GAN-based approaches for ECG generation are proposed by Neifar *et al.* [24, 22]. In these approaches, authors proposed automated solutions to leverage shape prior knowledge on ECG into the generation process by using a set of anchors [24] and 2-D statistical modeling [22]. A comparative study of these two methods is proposed in [23]. However, due to its adversarial training nature, the GAN architecture's principal drawbacks are training instability and limited generation diversity. Diffusion models, on the other hand, have recently emerged as a successful alternative, with demonstrated benefits over GANs in terms of training stability and superior generation qualities [3, 4, 16]. These models have been applied effectively in various applications, including time series generation and completion.

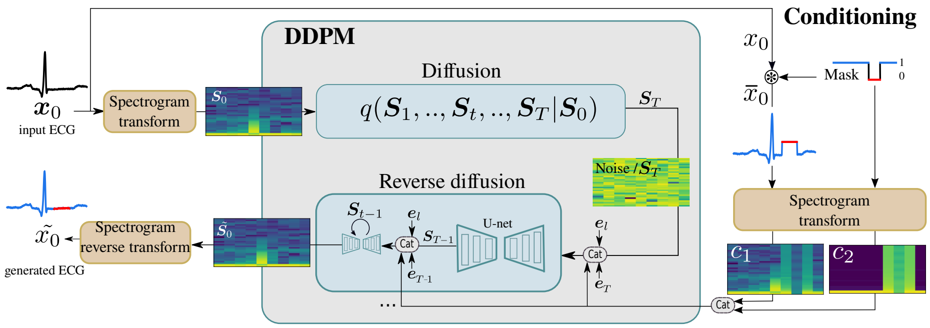

Fig. 1: The general principle of the proposed approach. Switching between the three tasks is implicitly done by defining the appropriate mask.

2.2 Principle of diffusion models

Diffusion models are a class of generative models that involve two Markovian processes: a diffusion process (*i.e.,* forward process) and a reverse diffusion process (*i.e.,* backward process). Gaussian noise is gradually added to the input data $\boldsymbol{x}_0 \sim q(\boldsymbol{x}_0)$ during the forward process over T steps according to a variance schedule $\beta \in [\beta_1, \beta_T]$ until the input distribution converge to a standard Gaussian distribution $q(\boldsymbol{x}_T) \sim \mathcal{N}(\boldsymbol{x}_T; 0, I)$. In the reverse diffusion process, a parameterized neural network θ is trained to remove the noise. The forward process is defined as :

$$q(\boldsymbol{x}_1, .., \boldsymbol{x}_t, .., \boldsymbol{x}_T | \boldsymbol{x}_0) = \prod_{t=1}^{T} q(\boldsymbol{x}_t | \boldsymbol{x}_{t-1}) \tag{1}$$

where $q(\boldsymbol{x}_t | \boldsymbol{x}_{t-1}) := \mathcal{N}(\boldsymbol{x}_t; \sqrt{1-\beta_t}\boldsymbol{x}_{t-1}, \beta_t I)$. The sampling of $\boldsymbol{x}_t$ can be described in closed form as $\boldsymbol{x}_t = \sqrt{\bar{\alpha}_t}\boldsymbol{x}_0 + (1-\bar{\alpha}_t)\epsilon$, where $\epsilon \sim \mathcal{N}(0,1)$, $\alpha_t = 1-\beta_t$ and $\bar{\alpha}_t = \prod_{i=1}^{t} \alpha_i$. The backward process learns to reverse this noising process to retrieve $\boldsymbol{x}_0$ from $\boldsymbol{x}_t$. Starting with the pure Gaussian noise sampled from $p(\boldsymbol{x}_T) := \mathcal{N}(\boldsymbol{x}_T, 0, I)$, the reverse process is described by a Markov chain as follows:

$$p_\theta(\boldsymbol{x}_{0:T}) = p(\boldsymbol{x}_T) \prod_{t=1}^{T} p_\theta(\boldsymbol{x}_{t-1} | \boldsymbol{x}_t) \tag{2}$$

By defining a specific parametrization of $p_\theta(\boldsymbol{x}_{t-1} | \boldsymbol{x}_t)$, Ho *et al.* [11] showed that the reverse process can be trained using the following objective:

$$L = min_\theta E_{\boldsymbol{x}_0 \sim D, \epsilon \sim \mathcal{N}(0,1), t \sim U(0,T)} \|\epsilon - \epsilon_\theta(\sqrt{\alpha_t}\boldsymbol{x}_0 + (1-\alpha_t)\epsilon, t)\|_2^2 \tag{3}$$

where the denoising function ϵ_θ estimates the noise ϵ added to get the noisy input $\boldsymbol{x}_t$.

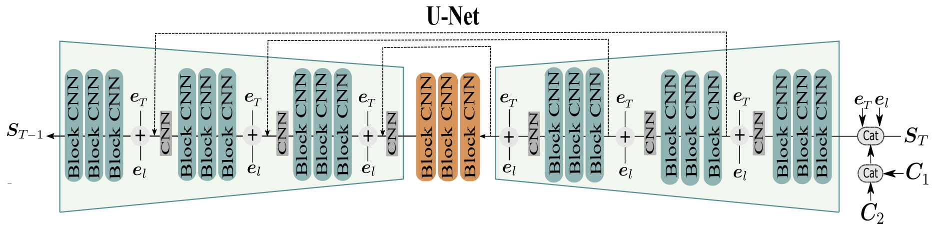

Fig. 2: Details of the U-Net architecture used for one denoising step.

3 Proposed Approach

The general principle of our proposed approach is depicted in Figure 1, which involves transferring the input ECG signal vector $\boldsymbol{x}_0$ from time domain to frequency domain to obtain spectrogram matrix denoted by $\boldsymbol{S}_0$. This transformation is performed to leverage the success of diffusion models in image generation.

During the training phase, we apply a diffusion process on the spectrogram $\boldsymbol{S}_0$, where noise is added gradually to it, resulting in the noisy spectrogram $\boldsymbol{S}_T$. For the reverse process, we adapted the U-Net architecture [25]. In previous research works, the U-Nets have been successfully employed and proven their effectiveness as model architecture in diffusion models in images generating [5].

During reverse diffusion process, $\boldsymbol{S}_T$ is first concatenated to the class embedding label $\boldsymbol{e}_l$ of $\boldsymbol{x}_0$ and the time step embedding $\boldsymbol{e}_T$. Moreover, we introduce $\boldsymbol{C}_1$ and $\boldsymbol{C}_2$, two additional conditions relative to the ECG prior shape in case of completion or forecasting to guide the reverse process. $\boldsymbol{C}_1$ is the spectrogram of the masked signal, where only masked random portions in the signal are set to 0. $\boldsymbol{C}_2$ is the spectrogram of the used mask. The resulting concatenated tensor is then fed to our U-Net model to remove the noise added in step T and generate a less noisy spectrogram $\boldsymbol{S}_{T-1}$. The process is repeated over the T steps to get the new spectrogram $\tilde{\boldsymbol{S}}_0$. Figure 2 presents the architecture of the U-net model used for the denoising step. This iterative reverse process can be formulated as follows:

$$p_\theta(\boldsymbol{S}_{0:T}|l, \boldsymbol{C}_1, \boldsymbol{C}_2) = p(\boldsymbol{S}_T) \prod_{t=1}^{T} p_\theta(\boldsymbol{S}_{t-1}|\boldsymbol{S}_t, l, \boldsymbol{C}_1, \boldsymbol{C}_2) \tag{4}$$

Finally, we apply a spectrogram reverse transform to $\tilde{\boldsymbol{S}}_0$ to produce the generated ECG signal $\tilde{\boldsymbol{x}_0}$.

To enhance the convergence of the reverse diffusion in completion and forecasting tasks, we consider an MSE regression loss computed between generated and ground truth signals. This is in addition to the reverse diffusion loss previously detailed in equation 3.

4 Experimental evaluation

This section presents the used dataset, details our model training settings, presents the conducted experiments and discusses obtained results.

4.1 Dataset

To train our model, we use the MIT-BIH arrhythmia database, which is widely recognized as the standard dataset for arrhythmia detection and classification [21]. This dataset contains 48 half-hour ECG recordings of different patients examined at the BIH Arrhythmia Laboratory between 1975 and 1979. Each recording consists of two annotated 30-minute ECG leads, digitally recorded at 360 samples per second. This dataset includes more than 100,000 ECG heartbeats. The majority of them belong to the normal ECG. A typical ECG heartbeat consists of distinct waves (P wave, a QRS complex, and a T wave). For ECG generation, three classes of heartbeats are usually taken into consideration: the normal beats, the premature ventricular contraction beats, and fusion beats (classes N, V, and F respectively).

4.2 Training settings

To implement our model, we used the PyTorch library and trained it on an Ubuntu server equipped with a GeForce GTX 1080 ti GPU with 11 GB of memory. The ADAM algorithm with a learning rate of 0.001 was used for stochastic gradient optimization. The number of steps in the diffusion process was set to 1000, while the minimum of schedule noise is $\beta_0 = 0.0001$ and the maximum is $\beta_T = 0.02$. We used torchaudio library for transferring modalities between ECG signals and their spectrograms, in both forward and reverse directions. An ECG signal is divided into heartbeats, also known as cardiac cycles, with each heartbeat consisting of 270 voltage values. A cardiac cycle is therefore a vector with a length of 270 values, corresponding to 350 and 400 milliseconds before and after the R-peak. we randomly chose 70% of the data for the training steps, while the remaining 30% of the data was used for models testing.

4.3 Experiments and results

Two steps of evaluation were considered to evaluate our approach: a quantitative and qualitative evaluations.

In the qualitative evaluation, we start with determining the impact of augmenting the real training dataset with additional synthetic data generated by our approach on the performance of stat-of-art arrhythmia classification baselines. We also compared the performance of our generation method with other competing generation approaches. Additionally, we used various standard metrics to quantitatively evaluate our approach in the three considered scenarios, generation, completion and forecasting.

As a qualitative evaluation, we visually checked the generated ECG signals for the different scenarios to identify any inconsistencies and visual incoherence.

Quantitative evaluation

Classification evaluation: In this evaluation, we used three stat-of-art arrhythmia classification baselines [15, 13, 1] to assess the impact of adding synthetic data obtained by different generation methods. As a first generation baseline, we adapted the seminal GAN work [9] to our context. We considered also two other recent GAN-based ECG generation methods [24, 22] that successfully incorporate shape prior to guide the generation process leading to prominent results.

The training of arrhythmia classifiers [15, 13, 1] was performed following 5 different settings:

- Setting 1: only the real training dataset is used to train the classifiers.
- Setting 2: training dataset is augmented by synthetic ECG generated by [9].
- Setting 3: training dataset is augmented by synthetic ECG generated by [24].
- Setting 4: training dataset is augmented by synthetic ECG generated by [22].
- Setting 5: training dataset is augmented by synthetic ECG generated by our approach.

In settings 2, 3, 4 and 5, the training datasets are augmented by 3000% of synthetic data for all three ECG classes.

Table 1: Classification results for [1] for the different settings.

	Accuracy	Precision	Recall	F1 score
Setting 1	0.97	0.93	0.89	0.91
Setting 2	0.98	0.94	0.91	0.92
Setting 3	0.98	0.95	0.93	0.94
Setting 4	0.99	0.97	0.95	0.94
Setting 5	0.99	0.95	0.93	0.94

Table 2: Classification results for [15] for the different settings.

	Accuracy	Precision	Recall	F1 score
Setting 1	0.98	0.87	0.82	0.84
Setting 2	0.98	0.93	0.91	0.92
Setting 3	0.98	0.96	0.94	0.95
Setting 4	0.99	0.97	0.95	0.96
Setting 5	0.99	0.96	0.95	0.95

Table 3: Classification results for [13] for the different settings.

	Accuracy	Precision	Recall	F1 score
Setting 1	0.96	0.87	0.74	0.77
Setting 2	0.97	0.87	0.79	0.82
Setting 3	0.99	0.96	0.95	0.95
Setting 4	0.99	0.96	0.96	0.96
Setting 5	0.99	0.94	0.95	0.95

Tables 1, 2, and 3 show the obtained classification results for the different settings. We can observe that adding synthetic ECG in the training phase systematically improves the arrhythmia classification performances of the three baselines. Moreover, our generation method outperforms the standard GAN [9] and achieves comparable results to the most advanced GAN-based approaches [24, 22]. It is worth to notice that these approaches are used only for data generation. However, our method is a generalized approach adapted for generation, completion and forecasting without any fine-tuning and reconfiguration.

Evaluation metrics: Following previous studies [10, 30, 28], we consider the Mean Squared Error (MSE), Root Mean Squared Error (RMSE), Mean Absolute Error (MAE), Fréchet Inception Distance (FID), Chamfer distance (CD), Earth Mover's Distance (EMD) and Maximum Mean Discrepency (MMD) as performance metrics.

We first present the obtained metrics for the generation task, followed by a comparison with the metrics obtained for the completion and forecasting tasks.

Table 4 reports the values of the used metrics for ECG generation approaches, where an amount of 1000 samples from both real data and synthetic data was selected. For all metrics, lower scores mean good results. Overall, our method produces results that are competitive with the three other competing generation methods. For example, we obtained 4.51e-4 for RMSE which is comparable to (9.48e-4, 4.34e-4,4.23e-4) in ([9], [24] and [22]), respectively. However, we clearly outperform them on the metrics MAE, FID and MMD as we obtained for example 2.90e-4 for MAE, while ([9], [24] and [22]) obtained (6.16e-4, 3.10e-4, and 3.02e-4), respectively.

Table 5 shows the obtained results of the used metrics for the completion and forecasting tasks, respectively. We can observe that our method achieves better results for all metrics in completion and forecasting tasks relatively to the generation task. This improvement can be attributed to the additional use of an MSE regression loss when training completion and forecasting tasks.

Qualitative evaluation For the qualitative assessment, we select random heartbeats and compare them with the distribution of the training dataset. Figure 3(a) shows examples of synthetic heartbeats from classes (N, V, and F), alongside the real distribution of these classes. The generated heartbeats exhibit realistic morphology and closely follow the real distribution. Figure 3(b and c) present examples of heartbeats with two missing values scenarios in the three classes. Our method accurately completes the missing values in these heartbeats, demonstrating a high completion performance. Additionally, Figure 3(d) displays examples of heartbeats forecasting for classes (N, V, and F), showcasing our approach's ability to accurately forecast ECG signals with realistic morphology. Figure 4 presents the t-SNE visualisations for the class N (a), class V (b), and class F (c). We can see that the synthetic data have a significant overlap with the real data.

Table 4: Obtained results of quantitative metrics for generation task

	Class N	Class V	Class F	Overall (ours)	Overall [9]	Overall [24]	Overall [22]
MSE	1.49e-07	1.45e-06	2.76e-05	2.03e-07	8.99e-07	1.88e-07	1.79e-07
RMSE	3.86e-4	1.24e-04	5.26e-03	4.51e-4	9.48e-4	4.34e-4	4.23e-4
MAE	2.54e-4	8.47e-04	3.93e-3	**2.90e-4**	6.16e-4	3.10e-4	3.02e-4
FID	2.44e-3	7.77e-03	5.64e-2	**2.84e-3**	8.92e-3	6.34e-3	2.91e-3
CD	1.26e-05	9.67e-05	4.21e-3	1.61e-5	1.5e-4	5.19e-5	8.65e-6
EMD	2.61e-3	9.35e-3	6.1e-2	3.10e-3	1.1e-2	5.74e-3	2.3e-3
MMD	0.25	0.15	0.55	**0.17**	0.30	0.23	0.20

Table 5: Obtained results for our method for the completion and forecasting tasks.

	Completion			Forecasting		
	Class N	Class V	Class F	Class N	Class V	Class F
MSE	1.11e-07	1.41e-06	1.67e-05	1.22e-07	1.16e-07	1.46e-05
RMSE	3.33e-4	1.18e-03	4.09e-03	3.49e-4	1.07e-03	3.83e-03
MAE	2.215e-4	7.71e-04	2.80e-3	2.57e-4	6.99e-04	2.77e-3
FID	2.28e-3	7.13e-03	3.57e-2	2.22e-3	6.22e-03	2.74e-2
CD	8.68e-06	1.25e-04	2.50e-3	8.65e-06	7.33e-05	1.59e-3
EMD	2.35e-3	8.45e-3	3.46e-2	2.65e-3	6.92e-3	3.17e-2
MMD	0.24	0.14	0.27	0.26	0.11	0.27

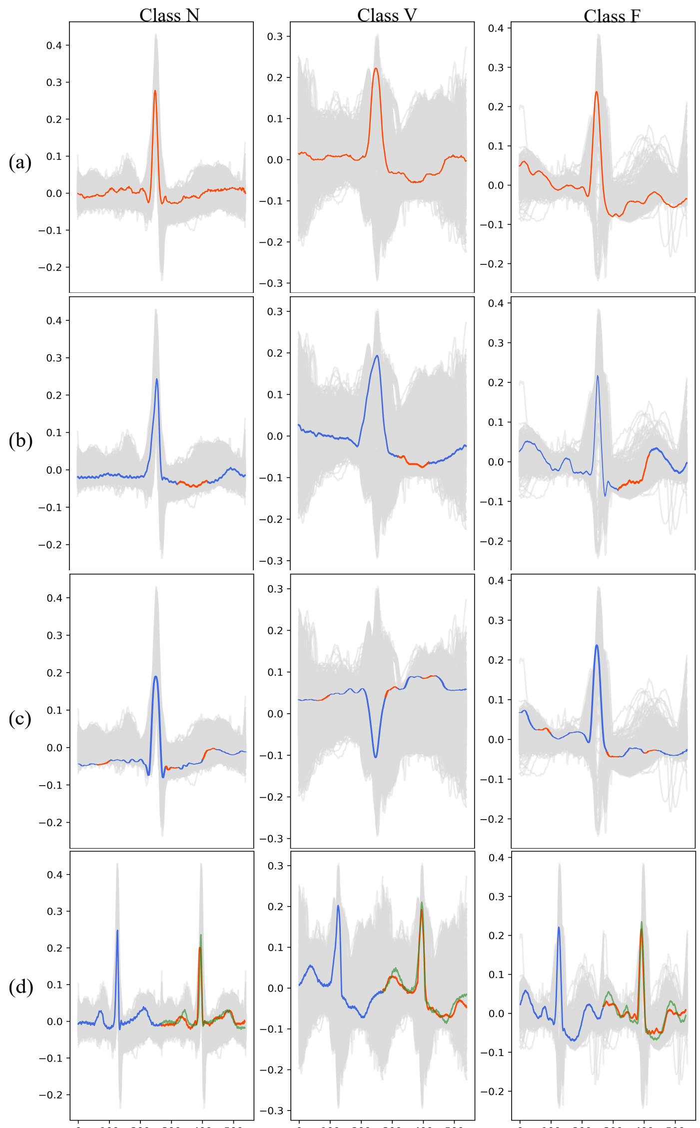

Fig. 3: Examples of synthetic heartbeats for classes N, V, and F classes obtained from the three tasks of generation (a), completion (b and c), and forecasting (d). The gray background represents the distribution of the real dataset, while the red portions depicts the heartbeats generated using our model. The blue and green portions represent the conditioning and ground truth, respectively.

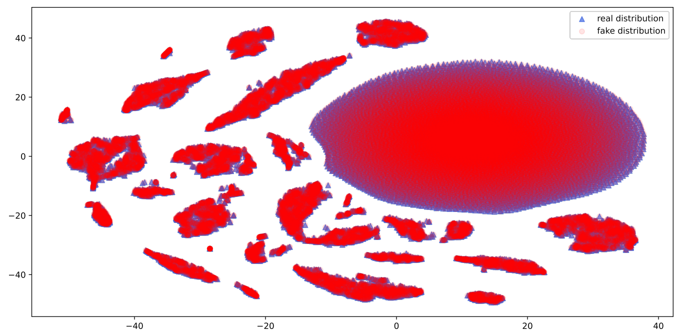

(a) class N

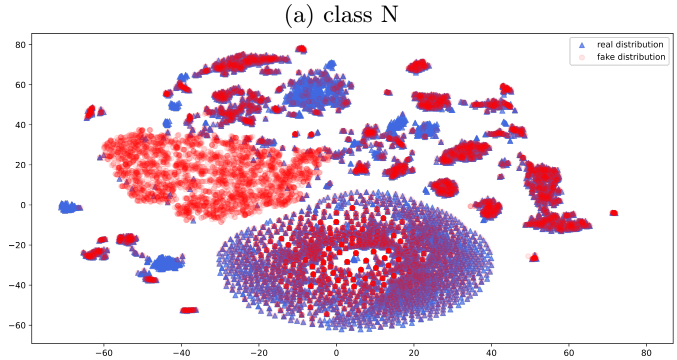

(b) Class V

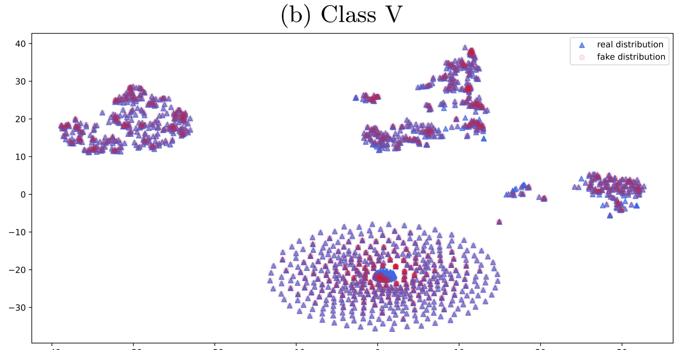

(c) Class F

Fig. 4: t-SNE visualisations for the class N (a), class V (b), and class F (c). The blue denotes real data, and red denotes synthetic data. We can see that the synthetic data have a significant overlap with the real data.

5 Conclusion

In this paper, we presented a first generalized conditional diffusion framework for ECG synthesis that can perform three different tasks: heartbeats generation, completion and forecasting. The obtained results demonstrated the effectiveness of our approach, as well as its ability to enhance state-of-the-art classifiers' performance. For future work, we plan to investigate the combination of diffusion models with adversarial training to further enhance ECG synthesis. Additionally, we aim to extend our approach to generate others classes of arrhythmia and multi-lead ECG signals. We plan also to cover other physiological signals.

References

1. Acharya, U.R., Oh, S.L., Hagiwara, Y., Tan, J.H., Adam, M., Gertych, A., San Tan, R.: A deep convolutional neural network model to classify heartbeats. Computers in biology and medicine **89**, 389–396 (2017)
2. Alcaraz, J.M.L., Strodthoff, N.: Diffusion-based time series imputation and forecasting with structured state space models. arXiv preprint arXiv:2208.09399 (2022)
3. Alcaraz, J.M.L., Strodthoff, N.: Diffusion-based time series imputation and forecasting with structured state space models. arXiv preprint arXiv:2208.09399 (2022)
4. Alcaraz, J.M.L., Strodthoff, N.: Diffusion-based conditional ecg generation with structured state space models. arXiv preprint arXiv:2301.08227 (2023)
5. Dhariwal, P., Nichol, A.: Diffusion models beat gans on image synthesis. In: Ranzato, M., Beygelzimer, A., Dauphin, Y., Liang, P., Vaughan, J.W. (eds.) Advances in Neural Information Processing Systems. vol. 34, pp. 8780–8794. Curran Associates, Inc. (2021)
6. Festag, S., Spreckelsen, C.: Medical multivariate time series imputation and forecasting based on a recurrent conditional wasserstein gan and attention. Journal of Biomedical Informatics **139**, 104320 (2023)
7. Golany, T., Freedman, D., Radinsky, K.: ECG ODE-GAN: Learning ordinary differential equations of ECG dynamics via generative adversarial learning. Proceedings of the AAAI Conference on Artificial Intelligence **35**, 134–141 (2021)
8. Golany, T., Radinsky, K.: PGANs: Personalized generative adversarial networks for ecg synthesis to improve patient-specific deep ECG classification. Proceedings of the AAAI Conference on Artificial Intelligence **33**(01), 557–564 (2019)
9. Goodfellow, I., Pouget-Abadie, J., Mirza, M., Xu, B., Warde-Farley, D., Ozair, S., Courville, A., Bengio, Y.: Generative adversarial nets. Advances in neural information processing systems **27**, 2672–2680 (2014)
10. Hazra, D., Byun, Y.C.: SynSigGAN: Generative adversarial networks for synthetic biomedical signal generation. Biology **9**(12), 441 (2020)
11. Ho, J., Jain, A., Abbeel, P.: Denoising diffusion probabilistic models. In: Larochelle, H., Ranzato, M., Hadsell, R., Balcan, M., Lin, H. (eds.) Advances in Neural Information Processing Systems. vol. 33, pp. 6840–6851. Curran Associates, Inc. (2020)
12. Ho, J., Salimans, T., Gritsenko, A.A., Chan, W., Norouzi, M., Fleet, D.J.: Video diffusion models. In: Oh, A.H., Agarwal, A., Belgrave, D., Cho, K. (eds.) Advances in Neural Information Processing Systems (2022)
13. Kachuee, M., Fazeli, S., Sarrafzadeh, M.: Ecg heartbeat classification: A deep transferable representation. In: 2018 IEEE International Conference on Healthcare Informatics (ICHI). pp. 443–444. IEEE (2018)

14. Kamaruddin, N.H., Murugappan, M., Omar, M.I.: Early prediction of cardiovascular diseases using ecg signal: Review. In: 2012 IEEE Student Conference on Research and Development (SCOReD). pp. 48–53 (2012). https://doi.org/10.1109/SCOReD.2012.6518609
15. Kumar, G., Pawar, U., O'Reilly, R.: Arrhythmia detection in ecg signals using a multilayer perceptron network. In: The 27th Irish Conference on Artificial Intelligence and Cognitive Science. pp. 353–364. AICS (2019)
16. Li, H., Ditzler, G., Roveda, J., Li, A.: Descod-ecg: Deep score-based diffusion model for ecg baseline wander and noise removal. IEEE Journal of Biomedical and Health Informatics (2023)
17. Li, X., Metsis, V., Wang, H., Ngu, A.H.H.: Tts-gan: A transformer-based time-series generative adversarial network. In: Michalowski, M., Abidi, S.S.R., Abidi, S. (eds.) Artificial Intelligence in Medicine. pp. 133–143. Springer International Publishing (2022)
18. Luo, Y., Zhang, Y., Cai, X., Yuan, X.: E$^{\mathbf{2}}$gan: End-to-end generative adversarial network for multivariate time series imputation. In: Proceedings of the Twenty-Eighth International Joint Conference on Artificial Intelligence, IJCAI-19. pp. 3094–3100. International Joint Conferences on Artificial Intelligence Organization (2019)
19. Mensah, G.A., Roth, G.A., Fuster, V.: The global burden of cardiovascular diseases and risk factors: 2020 and beyond. Journal of the American College of Cardiology **74**(20), 2529—2532 (November 2019)
20. Miao, X., Wu, Y., Wang, J., Gao, Y., Mao, X., Yin, J.: Generative semi-supervised learning for multivariate time series imputation. Proceedings of the AAAI Conference on Artificial Intelligence **35**(10), 8983–8991 (2021)
21. Moody, G., Mark, R., Goldberger, A.: Physionet: a web-based resource for the study of physiologic signals. IEEE Engineering in Medicine and Biology Magazine pp. 707–75 (2001)
22. Neifar, N., Ben-Hamadou, A., Mdhaffar, A., Jmaiel, M., Freisleben, B.: Leveraging statistical shape priors in gan-based ecg synthesis. arXiv preprint arXiv:2211.02626 (2022)
23. Neifar, N., Ben-Hamadou, A., Mdhaffar, A., Jmaiel, M., Freisleben, B.: A comparative study of GAN methods for physiological signal generation. In: Proceedings of the 12th International Conference on Pattern Recognition Applications and Methods, ICPRAM 2023, Lisbon, Portugal, February 22-24, 2023. pp. 707–714. SCITEPRESS (2023). https://doi.org/10.5220/0011794200003411
24. Neifar, N., Mdhaffar, A., Ben-Hamadou, A., Jmaiel, M., Freisleben, B.: Disentangling temporal and amplitude variations in ecg synthesis using anchored gans. In: The 37th ACM/SIGAPP Symposium on Applied Computing. pp. 645—-652. ACM (2022)
25. Ronneberger, O., Fischer, P., Brox, T.: U-net: Convolutional networks for biomedical image segmentation. In: Navab, N., Hornegger, J., Wells, W.M., Frangi, A.F. (eds.) Medical Image Computing and Computer-Assisted Intervention – MICCAI 2015. pp. 234–241. Springer International Publishing (2015)
26. Song, Y., Sohl-Dickstein, J., Kingma, D.P., Kumar, A., Ermon, S., Poole, B.: Score-based generative modeling through stochastic differential equations. In: International Conference on Learning Representations (2021)
27. Tashiro, Y., Song, J., Song, Y., Ermon, S.: Csdi: Conditional score-based diffusion models for probabilistic time series imputation. In: Ranzato, M., Beygelzimer, A., Dauphin, Y., Liang, P., Vaughan, J.W. (eds.) Advances in Neural Information Processing Systems. vol. 34, pp. 24804–24816. Curran Associates, Inc. (2021)

28. Xu, Q., Huang, G., Yuan, Y., Guo, C., Sun, Y., Wu, F., Weinberger, K.: An empirical study on evaluation metrics of generative adversarial networks. arXiv preprint arXiv:1806.07755 (2018)
29. Yoon, J., Jarrett, D., van der Schaar, M.: Time-series generative adversarial networks. In: Wallach, H., Larochelle, H., Beygelzimer, A., d'Alché-Buc, F., Fox, E., Garnett, R. (eds.) Advances in Neural Information Processing Systems. vol. 32. Curran Associates, Inc. (2019)
30. Zhu, F., Ye, F., Fu, Y., Liu, Q., Shen, B.: Electrocardiogram generation with a bidirectional LSTM-CNN generative adversarial network. Scientific Reports **9**(6734), 1–11 (2019)